Distributed Sliding Mode Control of pH in Tubular Photobioreactors

Gustavo A. de Andrade, Daniel J. Pagano, *Member, IEEE*, José Luis Guzmán, Manuel Berenguel, *Senior Member, IEEE*, Ignacio Fernández, and Francisco Gabriel Acién

***Abstract*— This paper describes the development of a distributed sliding mode control controller to regulate the pH of a tubular photobioreactor using the total inorganic carbon as the controlled variable of the process. The main purpose of the control system is to maintain the pH around a desired reference value and, at the same time, attenuate the undesirable transients caused by the disturbances. To study this problem, it is considered that this system is written as a set of hyperbolic partial differential equations. The distributed parameter model of the photobioreactor is transformed into a finite dimensional system by the method of characteristics. Then, the control design is performed in the finite dimensional system instead of the original distributed parameter model. The proposal allows to characterize the sliding regimes and their fundamental properties by a geometric approach. Through simulation and experimental results, the method is shown to be effective in controlling a tubular photobioreactor.**

***Index Terms*— Distributed parameter systems, method of characteristics, microalgae, pH control, sliding mode control (SMC), tubular photobioreactor.**

I. Introduction

MICROALGAE are a promising source of biomass for sustainable energy production. They can be extremely efficient in terms of land-use, as the potential oil productivity per hectare is considerably higher than traditional seed crops [1]. Until now, microalgae have been used with the purpose of obtaining high-value products mainly related to applications for humans and aquaculture [2]. Other microalgae applications include their use as biofilters to remove nutrients and other pollutants from wastewaters and as indicators for environmental change. Moreover, in some recent reviews [3], [4], the microalgae appear to be the only source of renewable biodiesel capable of meeting the global demand for transport fuels with potential to displace the fossil fuels dependence. Nonetheless, the costs associated with microalgae cultivation are high and they yield low profits. The worldwide production of microalgal biomass is 9000 t dry matter per year with a price ranging from 30 €/kg to 300 €/kg [5]. To be competitive in the bioenergy market, the microalgal production must become lower than 0.5 €/kg, much lower than actual cost [6].

Microalgae cultures have been traditionally cultivated in open raceway photobioreactors mainly due to their low costs and simplicity, but these photobioreactors have low operating control level and are susceptible to contamination. On the other hand, closed photobioreactors, for instance tubular photobioreactors, are preferred to produce high-value algal products, mainly from strains that cannot be cultivated in open ponds. This is achieved by adjusting the culture conditions to optimal values requested by microalgae strain used, especially pH.

In tubular photobioreactors, the pH is controlled by means of injection of pure carbon dioxide and helps to avoid carbon limitation enhancing the performance of the culture [7]. Depending of the control strategy, the costs associated with carbon dioxide represent 30% of the production costs [6]. Moreover, the carbon losses can be higher than 50% in extreme cases, and as consequence, a relevant amount of greenhouse gases are released into atmosphere, damaging the environment. A possible solution for this issue is to design advanced control strategies in order to regulate the pH of the culture, where the CO_2 losses can be reduced [8]. In this context, some control approaches have been proposed in the literature. For example, in [9] and [10], classic Proportional Integral (PI) controllers with feedforward scheme were developed based on simplified linear models of pH. In [11], a filtered Smith predictor strategy has been used to deal with photobioreactors with significant time delay due to pH sensor location. Even further, model-based predictive control strategies were also tested to regulate the pH in photobioreactors, such as the generalized predictive control (GPC) technique [8] or event-based GPC [12].

All these control techniques for pH control are based on simplified lumped linear parameter models. However, photobioreactors are characterized by disturbances, nonlinearities, uncertainties, and distributed parameters [partial differential equations (PDEs)]. Also, the dynamics of these plants is highly dependent upon the operating conditions, which can

Manuscript received July 11, 2015; accepted September 11, 2015. Manuscript received in final form September 16, 2015. Date of publication October 26, 2015; date of current version June 9, 2016. This work was supported in part by the Consejaría de Economía, Innovación y Ciencia de la Junta de Andalucía under Grant Control-Crop PIO-TEP-6174, in part by the Spanish Ministry of Economy and Competitiveness under Grant DPI2014-55932-C2-1-R, in part by the Spanish Ministry of Education under Grant PHB2009-0008, in part by Coordenação de Aperfeiçoamento de Pessoal de Nível Superior - Direção Geral de Universidades under Grant 220/2010, in part by the European Union–European Regional Development Fund. Funds under Grant DPI2014-56364-C2-1-R, and in part by the National Council for Scientific and Technological Development, Brazil. Recommended by Associate Editor E. Usai.

G. A. de Andrade and D. J. Pagano are with the Automation and Systems Department, Federal University of Santa Catarina, Florianópolis 88040-900, Brazil (e-mail: gustavo.artur@posgrad.ufsc.br; daniel.pagano@ufsc.br).

J. L. Guzmán, M. Berenguel, and I. Fernández are with the Informatics Department-Campus de Excelencia Internacional Agroalimentario–Centro de Investigación en Energía Solar, University of Almería, Almería E04120, Spain (e-mail: joseluis.guzman@ual.es; beren@ual.es; ifernandez@ual.es).

F. G. Acién is with the Chemical Engineering Department-CIESOL, University of Almería, Almería E04120, Spain (e-mail: facien@ual.es).

Color versions of one or more of the figures in this paper are available online at http://ieeexplore.ieee.org.

Digital Object Identifier 10.1109/TCST.2015.2480840

change widely. It is well known that neglecting the infinite dimensional nature of the original system may lead to a low control performance [13]. Therefore, it is desirable that the feedback control scheme implemented on such a process incorporates the mixing, mass transfer, and the spatial system dynamics to effectively operate in the whole operating range and to improve the microalgae growth performance.

Roughly speaking, there are two different scenarios in control of PDE systems (depending where the sensors and actuators are located):

1) boundary control [14], [15], where the actuator and sensing are applied only through the boundary conditions;
2) domain control [13], [16], where the actuation penetrates inside the domain of the PDE system or is distributed in the domain.

The photobioreactor treated in this paper corresponds to the second class above mentioned, where the actuation penetrates inside the domain of the system.

In this context, a sliding mode control (SMC) design approach, based on a first principle distributed parameter model [17], to regulate the pH of a tubular photobioreactor is proposed in this paper. The application of the SMC strategy in tubular photobioreactors is motivated by the improvement of the pH control to increase the photosynthesis rate and consequently the biomass productivity. The central idea of the proposal is the combination of the *method of characteristics* and SMC [18]. The method of characteristics is a mathematical technique to transform *hyperbolic* PDEs into a system of ordinary differential equations (ODEs), called *characteristic equations*. Then, the control design is performed based on these ODEs, which means that the results of ODEs control theory can be used to characterize sliding mode conditions of the original PDE system [19], [20]. Part of the results presented in this paper are contained in a preliminary form in [21] with only simulation results, where the control law is derived using the total inorganic carbon as the controlled variable. As will be shown, the studied photobioreactor is a system with relative degree 2, i.e., the output must be differentiated twice to generate an explicit relationship between the output and the input. However, it is well known that the classical *sliding condition* exists if and only if the system has a relative degree equal to 1 [22]. In order to overcome this problem, a new sliding condition, based on the ideas of [18] and [22]–[24], is developed in this paper to induce sliding regime in the photobioreactor system. Besides the conditions for sliding regime, the *reachability* and the *chattering* are another issues that need to be addressed in SMC strategies (see [25] for the classical concepts in SMC systems). These problems are resolved in this paper by applying a continuous control strategy derived from a candidate Lyapunov function.

The contributions of this paper are as follows. First, it is shown that it is possible to control the pH of the system using the total inorganic carbon as the controlled variable of the plant and using a nonlinear control approach (thus, obtaining more precise results than using linear control approaches, for instance, a classical PI controller). This hypothesis can be valid as carbon consumed by microalgae is compensated by supplying CO_2 to maintain pH and, as a consequence, a desired level of total inorganic carbon is achieved. A comparison by simulation of the proposed control system with a PI controller with feedforward scheme is presented, since this is the most common control scheme used. In addition, several performance indexes are calculated in order to provide a quantitative comparison between the two controllers. The performance of the proposed controller is also illustrated by means of experiments performed in an industrial plant.

Fig. 1. Real view of a tubular photobioreactor at the Las Palmerillas experimental station, Almería (Spain).

This paper is organized as follows. The tubular microalgal photobioreactor plant used in this paper is described in Section II. The SMC theory is presented in Section III. The experimental results are shown in Section IV. Some concluding remarks are summarized in Section V.

II. Tubular Photobioreactor

The tubular photobioreactor used in this paper to test the automatic control strategy is located at the Palmerillas Experimental Station, property of CAJAMAR foundation (Almería, Spain), located inside a greenhouse where the *Scenedesmus almeriensis* microalga is cultivated (see Fig. 1). This kind of microalga is characterized by a high growth rate, withstanding temperature up to 45 °C and pH values up to 10 [7]. The biomass is produced in continuous mode with a dilution rate of 0.34 L/day.

A general scheme of the plant is depicted in Fig. 2, showing the main components: 1) the external loop and 2) the bubble column.

The external loop is made of transparent tubes with 0.09 m diameter and joined into a loop configuration to obtain a total horizontal length of 400 m, with a capacity of 2200 L. The objective of the external loop is to increase the surface exposed to the sun in order for the microalgae to capture a larger amount of radiation and perform photosynthesis. Moreover, CO_2 in gas phase is injected at the beginning of the loop to provide the inorganic carbon to grow and to control the pH of the culture.

The bubble column is 3.25 m high and 0.5 m in diameter, with a capacity of 400 L, and performs several functions.

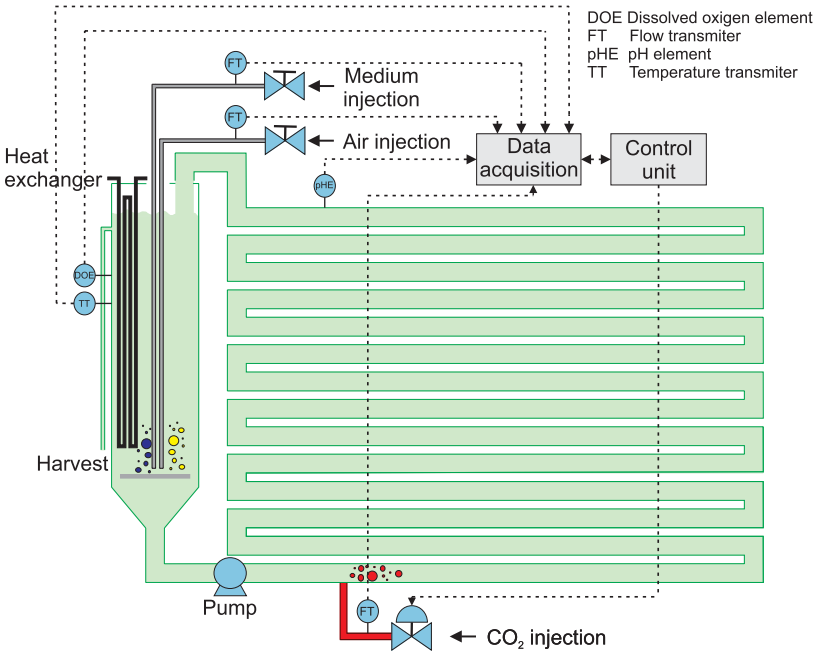

Fig. 2. Schematic of a tubular photobioreactor at the Las Palmerillas experimental station, Almería (Spain).

On one hand, it is used for mixing the culture and desorption of O_2 produced during the photosynthesis by air injection at a flow rate of 140 L/min. On the other hand, nutrients are also added in the column and the biomass harvesting is performed in this part of the process. The culture is continuously recirculated between the loop and the column using a pump located in the bottom of the column.

The pH, temperature, and dissolved oxygen are measured with Crison probes at several points of the solar receiver of the photobioreactor: three positions for dissolved oxygen and five positions for pH and temperature. These measurements are well distributed along the tube. The biomass concentration is estimated from a turbidity meter located at the bubble column. Moreover, liquid and gas flow rates are measured using digital flow meters. All these measurements are connected to a control computer through a data acquisition device National Instruments Compact FieldPoint.

A. Control Problem

The pH control problem in tubular photobioreactors deals with keeping the outlet pH of the external loop at a desired reference value in spite of disturbances. For this microalga specie, the optimal pH reference value is 8 [26].

The pH behavior in a microalgal culture is mainly influenced by two phenomena. On one hand, the intake of CO_2 as nutrient causes the formation of carbonic acid, leading to a decrease in the pH of the culture. On the other hand, when the microalgae perform the photosynthesis, they consume CO_2 and generate O_2, causing an increase in the pH. The provided CO_2 is transferred to the culture medium as a function of mass transfer coefficient in the system. Remaining fractions of injected CO_2 produce an oscillatory behavior in the measured pH, because of the continuous recirculation of the culture, until its total elimination.

The main system disturbances are the medium injected to perform the biomass harvesting, which introduces total inorganic carbon to the culture, and thus decreasing the pH value and solar irradiance changes, caused by the solar cycle and presence of clouds, produces changes in the rate of photosynthesis and thus in the rise of pH. The control variable is the CO_2 flow/velocity provided by a valve located at the beginning of the loop (see Fig. 2), which flow range is 0–5 L/min. In this paper, a control design based on controlling the total inorganic carbon is proposed. It must be stressed that this is not the only way to control this process. However, using the total inorganic carbon as controlled variable reduces the complexity of the calculus involved in the control law design if compared with directly using the pH variable for control design, due to the model equations. More details are given in the following sections.

B. Dynamic Model

The microalgal culture is a two-phase system and has been modeled by a set of coupled PDEs. In the liquid phase, biomass, dissolved oxygen, and total inorganic carbon concentrations mass balances are considered, while the gas phase takes into account the mass balance of carbon dioxide and oxygen molar fraction. The dynamic model of microalgal production of photobioreactors was previously developed and described in [17] and [27]. The photobioreactor used operates under atmospheric pressure, in which no significant overpressure existing in whatever place of the reactor. The flow is assumed to be 1-D. The reactor operates under controlled temperature conditions. The variation of temperature along the solar receiver is lower than 1 °C and ranging from 20 °C to 28 °C along the daily cycle, thus no large changes taking place. For this reason, the temperature balance is not considered in this

work. In the following, the photobioreactor model is briefly described. Note that the time and space variables are not explicitly written to save space and for readability.

The biomass mass balance is directly dependent on the photosynthesis rate, thus the equation for the biomass concentration is expressed as

$$\frac{\partial C_b}{\partial t} + V_l \frac{\partial C_b}{\partial x} = P_{\mathrm{O}_2} C_b Y_{p/x} \tag{1}$$

where $t \in [0, +\infty)$ is the time, $x \in [0, L]$ is the space, C_b is the biomass concentration, $Y_{p/x}$ is the biomass yield coefficient produced by the oxygen unit mass, $V_l = Q_l/(A(1-\varepsilon))$ is the liquid velocity, A is the cross-sectional area of the tube, ε is the gas holdup, and Q_l is the volumetric flow rate of liquid. The oxygen production rate per biomass mass unit is given by

$$P_{\mathrm{O}_2} = \frac{P_{\mathrm{O}_2\max} I_{\mathrm{av}}^n}{K_i \exp(I_{\mathrm{av}} m) + I_{\mathrm{av}}^n} \left(1 - \left(\frac{[\mathrm{O}_2]}{K_{\mathrm{O}_2}}\right)^z\right) \times \left(B_1 \exp\left(\frac{-C_1}{\mathrm{pH}}\right) - B_2 \exp\left(\frac{-C_2}{\mathrm{pH}}\right)\right) - r P_{\mathrm{O}_2\max}$$

where K_{O_2} is the oxygen inhibition constant, $[\mathrm{O}_2]$ is the dissolved oxygen concentration, $P_{\mathrm{O}_2\max}$ is the maximum photosynthesis rate for micro-organisms under the culture conditions, B_1 and B_2 are pre-exponential factors, C_1 and C_2 are the activation energies, I_{av} is the average solar irradiance, r is the respiration factor, and K_i, m, and z are form parameters.

Regarding the dissolved oxygen, this is related to the gas–liquid mass transfer rate and the photosynthesis rate as

$$\frac{\partial [\mathrm{O}_2]}{\partial t} + V_l \frac{\partial [\mathrm{O}_2]}{\partial x} = \frac{P_{\mathrm{O}_2} C_b}{M_{\mathrm{O}_2}} + K_{l a_l, \mathrm{O}_2}\left(\left[\mathrm{O}_2^*\right] - [\mathrm{O}_2]\right) \tag{2}$$

where M_{O_2} is the molecular weight of oxygen, $K_{l a_l, \mathrm{O}_2}$ is the volumetric gas–liquid mass transfer coefficient for oxygen, $[\mathrm{O}_2^*] = \mathrm{H}_{\mathrm{O}_2} P_T y_{\mathrm{O}_2}$ is the oxygen equilibrium concentration with gas phase, $\mathrm{H}_{\mathrm{O}_2}$ is the Henry's constant for oxygen, P_T is the total pressure, and y_{O_2} is the oxygen molar fraction in the gas phase.

The mass balance of the total inorganic carbon concentration is written in a similar way to the dissolved oxygen balance as

$$\frac{\partial [C_T]}{\partial t} + V_l \frac{\partial [C_T]}{\partial x} = \frac{P_{\mathrm{CO}_2} C_b}{M_{\mathrm{CO}_2}} + K_{l a_l, \mathrm{CO}_2}\left(\left[\mathrm{CO}_2^*\right] - [\mathrm{CO}_2]\right) \tag{3}$$

where $[C_T]$ is the total inorganic carbon concentration, $K_{l a_l, \mathrm{CO}_2}$ is the mass transfer coefficient for CO_2, $P_{\mathrm{CO}_2} = -P_{\mathrm{O}_2}$ is the carbon dioxide consumption rate, $[\mathrm{CO}_2^*] = \mathrm{H}_{\mathrm{CO}_2} P_T y_{\mathrm{CO}_2}$ is the dioxide carbon in equilibrium with the gas phase, $\mathrm{H}_{\mathrm{CO}_2}$ is Henry's constant for carbon dioxide, $[\mathrm{CO}_2]$ is the dissolved carbon dioxide, and y_{CO_2} is the carbon dioxide molar fraction in the gas phase.

The gas phase is made of CO_2 and O_2 molar fractions. The mass balance for carbon dioxide molar fraction is described as

$$\frac{\partial y_{\mathrm{CO}_2}}{\partial t} + V_g \frac{\partial y_{\mathrm{CO}_2}}{\partial x} = -\frac{V_{\mathrm{mol}}}{\varepsilon}(1-\varepsilon) K_{l a_l, \mathrm{CO}_2}\left(\left[\mathrm{CO}_2^*\right] - [\mathrm{CO}_2]\right) \tag{4}$$

where $V_g = Q_g/(A\varepsilon)$ is the gas phase velocity (control variable), Q_g is the volumetric flow rate of the gas, and V_{mol} the molar volume.

For the oxygen, an analogous mass balance can be established

$$\frac{\partial y_{\mathrm{O}_2}}{\partial t} + V_g \frac{\partial y_{\mathrm{O}_2}}{\partial x} = -\frac{V_{\mathrm{mol}}}{\varepsilon}(1-\varepsilon) K_{l a_l, \mathrm{O}_2}\left(\left[\mathrm{O}_2^*\right] - [\mathrm{O}_2]\right). \tag{5}$$

Equations (1)–(5) describe the photobioreactor state equations. In addition, a relationship between the total inorganic carbon concentration and the dissolved carbon dioxide in the culture is also needed for system closure. Such relationship is described as follows.

In microalgal cultures, the changes in pH are due mainly to consumption of carbon dioxide; pH variations due to consumption of other nutrients and degradation of excreted metabolites can be neglected [28]. As dioxide carbon in gas phase dissolves in the media, it breaks down into different species, namely, dissolved dioxide carbon, CO_2, carbonic acid $\mathrm{H_2CO_3}$, bicarbonate, $\mathrm{HCO_3^-}$, and carbonate $\mathrm{CO_3^{2-}}$. This chemical process can be described as follows. First, CO_2 reacts with water to yield carbonic acid

$$\mathrm{CO_2 + H_2O \leftrightarrow H_2CO_3}. \tag{6}$$

$\mathrm{H_2CO_3}$ is a weak acid and it dissociates, yielding $\mathrm{HCO_3^-}$

$$\mathrm{H_2CO_3 \leftrightarrow H^+ + HCO_3^-}. \tag{7}$$

The reaction equilibrium (7) can be described by an equilibrium constant K_1, expressed as

$$K_1 = \frac{\left[\mathrm{HCO_3^-}\right][\mathrm{H^+}]}{[\mathrm{CO_2}]} = 10^{-6.381}. \tag{8}$$

The $\mathrm{HCO_3^-}$ that is produced will further dissociate as

$$\mathrm{HCO_3^- \leftrightarrow H^+ + CO_3^{2-}}. \tag{9}$$

The dissociation (9) can also be described by a second equilibrium constant, K_2, such that

$$K_2 = \frac{\left[\mathrm{CO_3^{2-}}\right][\mathrm{H^+}]}{\left[\mathrm{HCO_3^-}\right]} = 10^{-10.377}. \tag{10}$$

Finally, the water dissociates according to

$$\mathrm{H_2O \leftrightarrow OH^- + H^+} \tag{11}$$

which is described by the following equilibrium constant:

$$K_w = [\mathrm{OH^-}] \cdot [\mathrm{H^+}] = 10^{-14}. \tag{12}$$

The $[\mathrm{H^+}]$ concentration is generally given as a pH value, defined as the negative logarithm, $\mathrm{pH} = -\log_{10}[\mathrm{H^+}]$.

The total inorganic carbon is equal to the sum of inorganic carbon species

$$[C_T] = [\mathrm{CO_2}] + \left[\mathrm{HCO_3^-}\right] + \left[\mathrm{CO_3^{2-}}\right]. \tag{13}$$

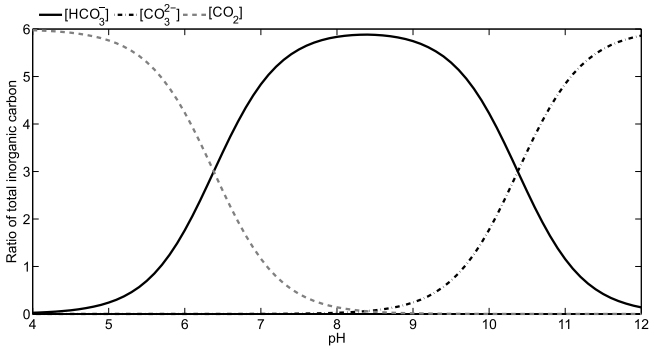

Fig. 3. Distribution of the forms of inorganic carbon in the photobioreactor with changes in pH.

Combining (8), (10), and (13), it is obtained

$$[C_T] = \left(1 + \frac{K_1}{[\mathrm{H}^+]} + \frac{K_1 K_2}{[\mathrm{H}^+]^2}\right)[\mathrm{CO}_2] \tag{14}$$

$$\frac{\partial [C_T]}{\partial t} = \left(1 + \frac{K_1}{[\mathrm{H}^+]} + \frac{K_1 K_2}{[\mathrm{H}^+]^2}\right)\frac{\partial [\mathrm{CO}_2]}{\partial t} - \left(\frac{K_1}{[\mathrm{H}^+]^2} + \frac{2K_1 K_2}{[\mathrm{H}^+]^3}\right)[\mathrm{CO}_2]\frac{\partial [\mathrm{H}^+]}{\partial t}. \tag{15}$$

In addition, the following electroneutrality constraint must be satisfied:

$$\frac{\partial [\mathrm{H}^+]}{\partial t} + \frac{\partial [\mathrm{Cat}^+]}{\partial t} = \frac{\partial [\mathrm{OH}^-]}{\partial t} + \frac{\partial [\mathrm{HCO}_3^-]}{\partial t} + 2\frac{\partial [\mathrm{CO}_3^{2-}]}{\partial t} + \frac{\partial [\mathrm{An}^-]}{\partial t}. \tag{16}$$

Assuming constant concentrations of cations, $[\mathrm{Cat}^+]$, and anions, $[\mathrm{An}^-]$, (16) is rewritten as

$$\frac{\partial [\mathrm{H}^+]}{\partial t} = \frac{\frac{K_1}{[\mathrm{H}^+]} + \frac{2K_1K_2}{[\mathrm{H}^+]^3}}{1 + \frac{K_w}{[\mathrm{H}^+]^2} + \frac{K_1[\mathrm{CO}_2]}{[\mathrm{H}^+]^2} + 2\frac{K_1K_2}{[\mathrm{H}^+]^3}}\frac{\partial [\mathrm{CO}_2]}{\partial t}. \tag{17}$$

If the chemical equilibria between the different forms are disturbed—as when dioxide carbon is added to the culture, removed in photosynthesis, or vented to the air—the reaction will shift one way or the other in an attempt to re-establish equilibrium. For example, when CO_2 is added to the system the H^+ increases following the production of H_2CO_3, as can be seen in (6) and (7). So, the pH decreases and consequently the total inorganic carbon rises. Conversely, when CO_2 is removed during photosynthesis or lost to the air by diffusion, the reactions shift to the left in (6) and (7). The H^+ concentration declines, but the CO_3^{2-} concentration slightly rises, preventing a rise in pH and a decrease in the total inorganic carbon concentration.

Fig. 3 shows the distribution of the forms of inorganic carbon in the photobioreactor with changes in pH in steady state. Note that at pH 6.5–10.5, bicarbonate is the most abundant form. CO_2 dominates at low pH, while carbonate dominates at high pH values.

As can be noted, if the pH is at an equilibrium point, the total inorganic carbon, with its inorganic carbons species, is at equilibrium too. In the case treated in this paper, carbon consumed by microalgae is compensated by supplying CO_2 to maintain pH and, as a consequence, a desired level of inorganic carbon is achieved. Based on this hypothesis, in this paper, the total inorganic carbon is used as output variable to control the pH.

In sum, the tubular photobioreactor model is given by (1)–(5), (15), and (17), which can be written in the following compact form:

$$\frac{\partial z}{\partial t} + \mathbf{A}(z(x,\, t))\frac{\partial z}{\partial x} = \mathbf{G}(z(x,t)) \tag{18}$$

where $z = [C_b, [\mathrm{O}_2], [C_T], [\mathrm{CO}_2], [\mathrm{H}^+], y_{\mathrm{CO}_2}, y_{\mathrm{O}_2}]$ $\mathbf{A}$ is a 7×7 matrix, and $\mathbf{G}$ is a vector function.

Since the controlled variable is the outlet total inorganic carbon of the external loop, the system output is defined as

$$y(t) = [C_T](t, L).$$

Regarding the boundary conditions, they are given at the entrance of the external loop to specify the inlet concentration values of the liquid and gas phase components, in which can be expressed by

$$z(0,\, t) = \boldsymbol{\phi}(t) \tag{19}$$

where $\boldsymbol{\phi}$ is a column vector. Moreover, the initial condition for model (18) is given by

$$z(x, 0) = \varphi(x), \quad 0 \le x \le L \tag{20}$$

where φ is a given C^1 function.

In this paper, it is assumed that the boundary conditions (19) and the initial condition (20) satisfy the conditions of C^1 compatibility (see [29]). Therefore, it can be guaranteed that there exists $\delta > 0$ such that system (18) with initial condition (20) and boundary conditions (19) is well-posed, i.e., it admits a unique local C^1 solution on the domain

$$\{(t,\, x) | 0 \le t \le \delta, 0 \le x \le L\}.$$

Questions related to the well-posedness of quasi-linear hyperbolic systems have been intensively studied in the literature. The interested reader is referred to [29] and [30] for more details.

1) Model in Terms of the Characteristic Equations: The photobioreactor model described in the previous section is a quasi-linear hyperbolic PDE system, i.e., for every x and t, the matrix $\mathbf{A}$ of (18) has real eigenvalues. Therefore, system (18) can be transformed into a set of first-order ODEs, called characteristic equations, by means of the method of characteristics. The basis of this transformation is the geometric analysis of the formation of surfaces from families of curves [30]. For the application of the method of characteristics, it suffices to consider (1)–(5) only, because the differential equations (15) and (17) are already in the desired form. This section is devoted to briefly present the transformation of the PDE system (18) into characteristic equations.

The left-hand side of (1)–(3) can be viewed as the directional time derivative of the unknown vector function z_i, $i = 1, \ldots, 3$, at a point (x, t) of the plane, along the curve having slope

$$\begin{aligned} \dot{x} &= V_l \\ \dot{t} &= 1 \end{aligned} \tag{21}$$

which implies that (1)–(3) can be written as

$$\begin{aligned}\dot{C}_b &= P_{\mathrm{O}_2} C_b Y_{p/x}\\ [\dot{\mathrm{O}}_2] &= \frac{P_{\mathrm{O}_2} C_b}{M_{\mathrm{O}_2}} + K_{l a_l,\mathrm{O}_2}\left(\left[\mathrm{O}_2^*\right] - [\mathrm{O}_2]\right)\\ [\dot{C}_T] &= \frac{P_{\mathrm{CO}_2} C_b}{M_{\mathrm{CO}_2}} + K_{l a_l,\mathrm{CO}_2}\left(\left[\mathrm{CO}_2^*\right] - [\mathrm{CO}_2]\right).\end{aligned} \tag{22}$$

It follows that the total inorganic carbon constraint (15) and electroneutrality (17) are rewritten as:

$$\begin{aligned}[\dot{\mathrm{CO}}_2] &= \frac{1}{P_2 - [\mathrm{CO}_2]P_1P_3}\\ &\quad\times\left[\frac{P_{\mathrm{CO}_2} C_b}{M_{\mathrm{CO}_2}} + K_{l a_l,\mathrm{CO}_2}\left(\left[\mathrm{CO}_2^*\right] - [\mathrm{CO}_2]\right)\right]\\ [\dot{\mathrm{H}}^+] &= \frac{P_3}{P_2 - [\mathrm{CO}_2]P_1P_3}\\ &\quad\times\left[\frac{P_{\mathrm{CO}_2} C_b}{M_{\mathrm{CO}_2}} + K_{l a_l,\mathrm{CO}_2}\left(\left[\mathrm{CO}_2^*\right] - [\mathrm{CO}_2]\right)\right]\end{aligned} \tag{23}$$

where

$$\begin{aligned}P_1 &= \frac{K_1}{[\mathrm{H}^+]^2} + \frac{2K_1K_2}{[\mathrm{H}^+]^3}\\ P_2 &= 1 + \frac{K_1}{[\mathrm{H}^+]} + \frac{K_1K_2}{[\mathrm{H}^+]^2}\\ P_3 &= \frac{\frac{K_1}{[\mathrm{H}^+]} + \frac{2K_1K_2}{[\mathrm{H}^+]^2}}{1 + \frac{K_w}{[\mathrm{H}^+]^2} + \frac{K_1[\mathrm{CO}_2]}{[\mathrm{H}^+]^2} + 4\frac{2K_1K_2}{[\mathrm{H}^+]^3}}.\end{aligned}$$

Similarly, (4)–(5) can be viewed as the directional time derivative of the unknown vector function z_j, $j = 6, 7$, at a point (x, t) along the curve defined by

$$\begin{aligned}\dot{x} &= V_g\\ \dot{t} &= 1.\end{aligned} \tag{24}$$

Along the curve (24), the following equations are satisfied:

$$\begin{aligned}\dot{y}_{\mathrm{O}_2} &= -\frac{V_{\mathrm{mol}}}{\varepsilon}(1-\varepsilon)K_{l a_l,\mathrm{O}_2}\left(\left[\mathrm{O}_2^*\right] - [\mathrm{O}_2]\right)\\ \dot{y}_{\mathrm{CO}_2} &= -\frac{V_{\mathrm{mol}}}{\varepsilon}K_{l a_l,\mathrm{CO}_2}\left(\left[\mathrm{CO}_2^*\right] - [\mathrm{CO}_2]\right).\end{aligned} \tag{25}$$

The curves defined by (21) and (24) are called *characteristic curves* and the system of ODEs (21)–(25) are called characteristic equations. In general, a closed solution of these equations cannot be found. Therefore, it is necessary to integrate them simultaneously using some numerical method. Note that on the region $0 < x \leq L$, the system solution is obtained from the characteristic equations (21)–(25), with initial condition (20). For the case where $x = 0$, the characteristic curves leave the domain. Therefore, the characteristic equations (21)–(25) are replaced by the boundary condition (19).

III. Distributed Sliding Mode Control

SMC was introduced in [31] as a method of discontinuous control for nonlinear systems. Basically, in this control approach, a surface must be designed in such a way that the system has some desired performance. A Lyapunov-like stability condition guarantees that the distance to the surface decreases along all system trajectories and constrains the trajectories to point toward the surface. The basic elements of this control strategy for lumped parameter systems can be seen in [25] and [32]. In this section, an approach for the photobioreactor distributed parameter model, called distributed SMC (DSMC), is presented following the ideas of [18]–[20]. The proposal uses the characteristic (22)–(25) for control design instead of the original PDE system. In this way, the well-known results for the description of sliding motions in lumped parameter systems become immediately available [19].

In the sequel, the control variable V_g will be called u, for sake of legibility. A variable structure feedback switching law is available to the controller as follows:

$$u = \begin{cases} u^+, & \text{if } h > 0\\ u^-, & \text{if } h < 0\end{cases} \tag{26}$$

where $u^+ > u^-$ and h is a scalar function of the states, so-called *switching boundary function*.

The condition $h = 0$ defines an isolated smooth manifold solution $[C_T] = \vartheta(x, t)$. It is assumed that the graph of ϑ is a smooth time varying surface with locally nonzero gradient. The zero level set of ϑ is labeled as *sliding surface* and is defined as

$$S = \{(z, x, t) \in \mathbb{R}^9 | h = 0\}. \tag{27}$$

Since the total inorganic carbon $[C_T]$ is the controlled variable and the gas velocity/flow V_g is the control variable, then the system's relative degree[1] is 2. The output variable $[C_T]$ must be differentiated twice to generate an explicit relationship between the output and the input [this can be seen by analyzing (3) and (4)]. It is well known that the classical theory of SMC just guarantees the sliding regime existence if and only if the system has a relative degree equal to 1 [22]. For this class of systems, it is sufficient to analyze the first-order time derivative of the sliding surface to determine the attractive sliding regime (see [33]). However, for systems with relative degree 2 this is not a sufficient condition, since the control variable does not appear in the first-order time derivative of the sliding surface. This is the case for the system studied in this paper. To deal with this problem, a second-order sliding manifold is developed to create a local sliding motion. For the following developments, it will be called κ_1 as the vector field generated by (21)–(23) and κ_2 as the vector field generated by (24) and (25).

Under switching control law (26), the characteristic equations (25) have two characteristic curves generated by the vector field κ_{2,u^+} and κ_{2,u^-}, respectively. It is referred to as κ_{2,u^+}, when $u = u^+$ is the control input and similarly κ_{2,u^-}, when $u = u^-$. The vector field κ_1 does not have any effect changing the control u from u^+ to u^-. Therefore, the characteristic curve associated with (22) is not defined for both values of the binary switching control law.

Basically, the controlled system has three different behaviors at the sliding surface: 1) crossing; 2) attractive sliding; and 3) repulsive sliding [21]. The main idea in sliding control system is to perform the following:

[1]A similar concept, called *characteristic index*, was introduced by Christofides and Daoutidis [13]. However, in this paper, the term relative degree is preferred over characteristic index.

1) to define the desired operating point (a stable pseudoequilibrium point) in such a way that it is in the attractive sliding region;
2) to guarantee that the system trajectories reach the surface from a defined local set of initial conditions.

Once the system trajectories are on this surface, they slide toward the pseudoequilibrium point and remain there. Note that the invariance condition $h = 0$ necessarily requires that $(dh/dt) = 0$. This last condition can be expressed in terms of the system trajectories by

$$L_{\kappa_1} h = 0 \tag{28}$$

where $L\kappa_1 h$ represents the Lie derivative of h with respect to the vector field κ_1

$$L_{\kappa_1} h = \dot{x}\frac{\partial h}{\partial x} + \frac{\partial h}{\partial t} + \dot{C}_b\frac{\partial h}{\partial C_b} + [\dot{\mathrm{O}}_2]\frac{\partial h}{\partial [\mathrm{O}_2]} + [\dot{C}_T]\frac{\partial h}{\partial [C_T]} + [\dot{\mathrm{CO}}_2]\frac{\partial h}{\partial [\mathrm{CO}_2]} + [\dot{\mathrm{H}}^+]\frac{\partial h}{\partial [\mathrm{H}^+]} \tag{29}$$

where $\dot{x}$, $\dot{C}_b$, $[\dot{\mathrm{O}}_2]$, $[\dot{C}_T]$, $[\dot{\mathrm{CO}}_2]$, and $[\dot{\mathrm{H}}^+]$ are directly obtained from (22).

As before mentioned, the vector κ_1 does not depend of the control variable u. Therefore, it is not possible to induce the system trajectories to the sliding surface $h = 0$ by directly acting on the vector field κ_1. In order to solve this problem, a new boundary function must be defined as the tangency set of the vector field κ_1 with $h = 0$, i.e., $L_{\kappa_1} h = 0$. The attractive sliding conditions are now defined on the vector field κ_2

$$L_{\kappa_{2,u^+}}(L_{\kappa_1} h) < 0, \quad \text{if } h > 0 \tag{30}$$

$$L_{\kappa_{2,u^-}}(L_{\kappa_1} h) > 0, \quad \text{if } h < 0 \tag{31}$$

where $L_{\kappa_{2,u^+}}(L_{\kappa_1} h)$ represents the Lie derivative of $(L_{\kappa_1} h)$ with respect to the vector field κ_{2,u^+} and $L_{\kappa_{2,u^-}}(L_{\kappa_1} h)$ represents the Lie derivative of $(L_{\kappa_1} h)$ with respect to the vector field κ_{2,u^-}. For sake of brevity, these expressions were omitted in this paper. Evidently, $(\partial/\partial u)[L_{\kappa_2,u}(L_{\kappa_1} h)] \neq 0$, therefore, an attractive sliding regime can be locally created on an open set $\mathcal{M}$ of S for a system with relative degree 2.

In sum, the idea of this methodology is to induce the vector field κ_2 by means of the feedback switching controller (26) to the hypersurface $L_{\kappa_1} h = 0$, which is contained in $h = 0$. In this way, it becomes possible to indirectly induce the vector field κ_1 to $h = 0$, since the vector fields κ_1 and κ_2 are coupled.

For all initial conditions of the system located on a vicinity of the attractive sliding surface, the unique control function, u_{eq}, locally constraining the system trajectories to the open set $\mathcal{M}$ of S is known as the *equivalent control*. The equivalent control turns the open set $\mathcal{M}$ of S into a local integral manifold of the controlled vector field. According to Filippov's method [34], the dynamics ideally constrained to $\mathcal{M}$ is named as the *ideal sliding dynamics*. Since $\mathcal{M}$ locally becomes an integral manifold, it follows that the gradient of $L_{\kappa_1} h$ is orthogonal to the controlled vector field κ_2:

$$L_{\kappa_{2,u_{\mathrm{eq}}}}(L_{\kappa_1} h) = 0 \tag{32}$$

where $\kappa_{2,u_{\mathrm{eq}}}$ stands for the ideal sliding dynamics induced by the interactions of the two vector fields κ_{2,u^+} and κ_{2,u^-}. Note that this orthogonality condition also implies that the gradient of h is orthogonal to the vector field κ_1. The equivalent control is given by the solution of (32) for u_{eq}, which is derived on the nominal system dynamics, and is effective only once the attractive sliding region is reached.

In [19], it has been shown that if the problem is well-posed, the attractive sliding regime will exist for the closed-loop system. Furthermore, the switching control law (26) must satisfy the reaching condition [25] to achieve the attractive sliding region in a finite time. This methodology, however, leads to the chattering phenomenon in the control action and in the controlled variable, which degrades the system performance. A possible solution to guarantee the reachability of the system to the sliding surface and, at the same time, to reduce the chattering problem is to design a continuous control law as

$$u = u_{\mathrm{eq}} + u_N \tag{33}$$

where u_N is the control action designed for the reaching phase during which the system trajectories starting off the sliding surface moves toward it, and u_{eq} is the control component that acts when the system is on the attractive region of the sliding surface [32]. In what follows, a methodology, based on a candidate Lyapunov function, to obtain such control law is described.

Let $V = (1/2)h^2$ be a candidate Lyapunov function. If the function dV/dt is negative definite, then the system trajectories will decrease until they reach the sliding surface. Evaluating such operation results in

$$\frac{dV}{dt} = h\frac{dh}{dt} < 0$$

or in terms of Lie derivative of the function h with respect to the vector field κ_1

$$\frac{dV}{dt} = h(L_{\kappa_1} h) < 0. \tag{34}$$

Taking $L_{\kappa_1} h = -\lambda_1 h$, with $\lambda_1 > 0$, the above inequality is satisfied. However, due to the fact that $(\partial/\partial u) L_{\kappa_1} h = 0$, it is not possible to directly impose $L_{\kappa_1} h = -\lambda_1 h$ by a control action. In order to tackle this problem, it is considered $V = 1/2(L_{\kappa_1} h + \lambda_1 h)^2$ as a new candidate Lyapunov function. The time derivative of this Lyapunov function with respect to the vector field κ_2 is

$$\frac{dV}{dt} = (L_{\kappa_1} h + \lambda_1 h)(L_{\kappa_{2,u}}(L_{\kappa_1} h + \lambda_1 h)) < 0. \tag{35}$$

Choosing $(L_{\kappa_{2,u}}(L_{\kappa_1} h + \lambda_1 h)) = -\lambda_2(L_{\kappa_1} h + \lambda_1 h)$, with $\lambda_2 > 0$, it is easy to see that inequality (35) is satisfied. Since $(\partial/\partial u)(L_{\kappa_{2,u}}(L_{\kappa_1} h + \lambda_1 h)) \neq 0$, this condition can be achieved by solving the following equation for u:

$$(L_{\kappa_{2,u}}(L_{\kappa_1} h + \lambda_1 h)) + \lambda_2(L_{\kappa_1} h + \lambda_1 h) = 0. \tag{36}$$

Again, it is easy to see that solving (36) for u will result in a smooth control law of the form (33), where λ_1 and λ_2 are design parameters that directly influence in the reaching condition of the system to the sliding surface. Although this smooth control law depends on the model parameters, it has robustness properties whenever λ_1 and λ_2

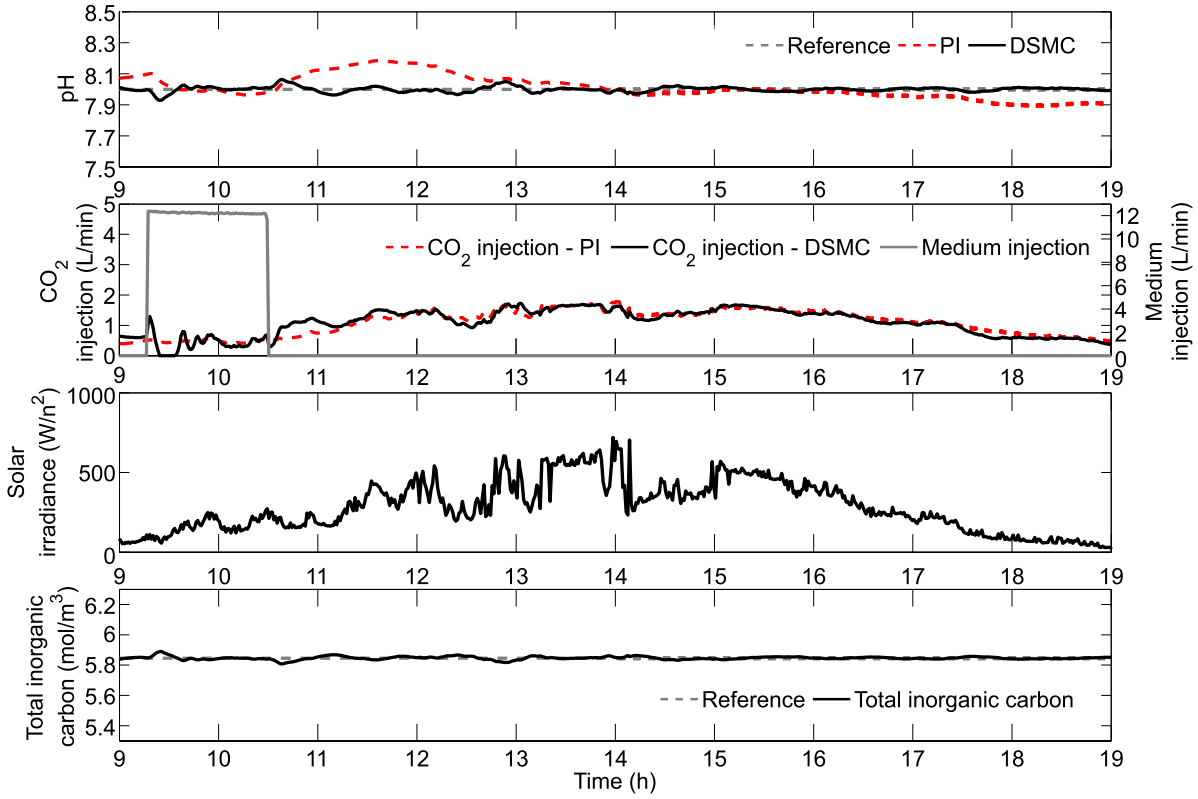

Fig. 4. Comparison of the simulation results between the DSMC and PI controller with feedforward scheme under real disturbances data.

are adequately tuned. The detailed derivation of the explicit control law for the photobioreactor system can be found in the Appendix, resulting in (45).

IV. Results

This section shows simulation and real experiments using the DSMC strategy, in which the control law is given by (44), applied to pH control in tubular photobioreactors. First, the DSMC strategy was tested in simulation and compared with a classic PI controller, where the model presented in Section II-B was used as virtual plant. All data used in simulations were collected from the real photobioreactor operating in continuous mode. The objective of this comparative study is to highlight the benefits that can be achieved using an advanced control strategy to regulate the pH of the photobioreactor. Afterward, the proposed control system is tested through real experiments on the industrial tubular photobioreactor described in Section II. In both simulation and real experiments, the pH set-point is set to 8, since this is the optimal value for the microalga strain used in this paper, and the maximal deviation is ± 0.075 in order to keep the optimal photosynthesis rate.

It must be stressed that for the numerical simulations, system (18) was used, and not the characteristic (22)–(25). The method of characteristics was used only to derive the control law.

A. Simulation Results

In this section, a comparison of the proposed controller with a PI controller with feedforward scheme is performed. For the simulation results shown here, it was considered that all state variables are being measured in the photobioreactor and are available for the controllers. Moreover, only the nominal case has been considered, and the total inorganic carbon set-point was obtained from the curve shown in Fig. 3. Some comments about the implementation of the proposed controller for systems, in which not all the state variables are measured, are given in Section IV-B.

The DSMC controller was implemented with $\tilde{\lambda}_1 = 128$, $\tilde{\lambda}_2 = 126$, and $T_i = 600$ s. For the PI controller with feedforward scheme, the same parameters as those proposed in [27] were used. Finally, the sampling time of both control systems is 60 s.

Fig. 4 shows the response of the DSMC controller and that of the PI controller with feedforward scheme for a representative day with rapid changes in solar irradiance. Fig. 4 shows the simulation test where the behavior of the two control schemes, with disturbance rejection capabilities, can be observed. The PI controller tracks the pH reference with small oscillations around the reference due to the poor compensation of the solar irradiance and dilution process disturbances, where fresh medium is injected in the photobioreactor. The fresh medium directly influences in the pH response, because the dilution process introduces total inorganic carbon. On the other hand, the DSMC controller adequately compensates for the disturbances caused by the solar irradiance transients and the dilution process of the system. Moreover, note in the bottom graph of Fig. 4 that the output variable of the proposed control strategy, the total inorganic carbon, is maintained constant

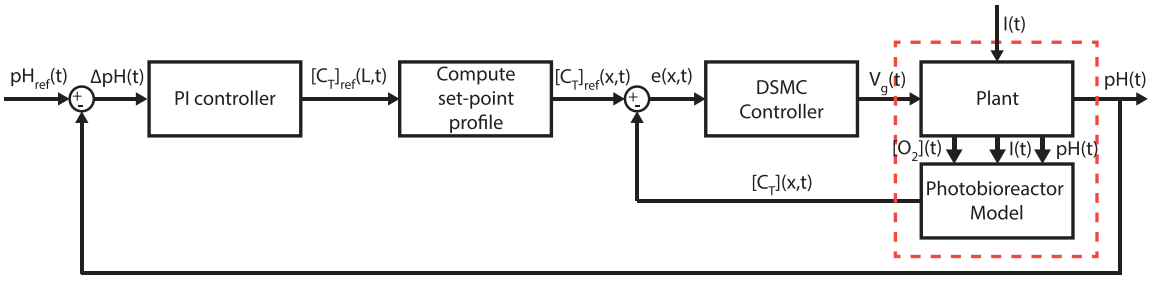

Fig. 5. Block diagram of control structure.

TABLE I
PERFORMANCE INDEXES CALCULATED TO THE DSMC AND PI CONTROLLERS IN SIDR AND MIDR DISTURBANCES REJECTION CAPABILITIES

		Case study	
		SIDR	MIDR
DSMC controller	IAE	8.08	8.11
	ITAE	1.76	1.63
	ISE	0.15	0.18
	ITSE	3.06	2.90
PI controller	IAE	53.00	45.39
	ITAE	13.37	11.75
	ISE	5.49	4.51
	ITSE	137.04	111.61

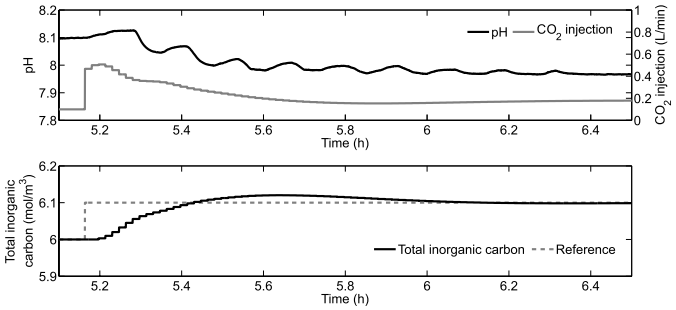

Fig. 6. Time-response dynamics of the total inorganic carbon, the CO_2 injection, and the pH when a step change at the total inorganic carbon reference was applied.

along the simulation in such a way that the pH tracks the desired reference.

To analyze the controller responses, their performance was characterized using the following indexes: integral of the square error, integral of time-weighted square error, integral of the absolute error, and integral of the time-weighted absolute error for medium injection disturbances rejection (MIDR) and solar irradiance disturbances rejection (SIDR) capabilities. Table I shows the performance indexes calculated for the two controllers. As can be observed, the DSMC controller performance overcomes the PI controller with feedforward scheme under the same conditions. Note in the top graph of Fig. 4 that the deviation of pH using the PI controller is greater than ± 0.075. Therefore, it can be deduced that microalgae growth performance is improved using the proposed control strategy, since it keeps the system closer to its optimal operation condition than the PI controller with feedforward scheme.

B. Experimental Results

This section shows the results obtained when using the proposed sliding mode controller to control the pH in the photobioreactor. The controller was implemented on an industrial computer located at the plant facility. A LabVIEW-based software executes the DSMC strategy, which was coded in the MATLAB environment. All systems sensors and actuators are connected to a Compact-FieldPoint unit from National Instruments. In such configuration, the controller node communicates with Compact-FieldPoint through a dedicated Ethernet network to perform sensing and control tasks.

The DSMC algorithm was implemented with the same parameters as in the simulation study. In addition, the implementation of the control law (44) contains a state observer to estimate the total inorganic carbon and the other variables present in the control law that are not measured in the real plant. This observer is based on the model (18)–(20) described in Section II-B. These equations were solved by the method of lines using a backward finite difference approximation. To ensure stability and to impose limits in the computational cost, the Courant–Friedricks–Lewy condition was used. Since this model was validated with real photobioreactor data with a discrepancy of around 1.2% between the values of the model states and the real system states [17], [27], no correction mechanism between the estimated state values and the real system states was used. Note that other effective approaches for state estimation could be used here, for instance, the work proposed in [16] on distributed state estimation, where a correction mechanism is used to enforce a fast decay of the discrepancy between the estimated and the actual values of the states of the system.

In addition to the DSMC controller, an outer feedback loop with integral action is used to calculate the total inorganic carbon concentration set-point required to maintain the system pH in its optimal value. The outer feedback loop is a PI controller with the following structure:

$$[C_T](L,t) = k_p\left(\Delta\mathrm{pH}(t) + \frac{1}{T_i}\int_0^t \Delta\mathrm{pH}(\tau)d\tau\right) \quad (37)$$

where $\Delta\mathrm{pH} = \mathrm{pH}_{\mathrm{ref}}(t) - \mathrm{pH}(t)$ and $\mathrm{pH}_{\mathrm{ref}}$ is the desired pH reference. The pH reference is kept in its optimal value during the experiments to guarantee maximal photosynthesis rate, i.e., $\mathrm{pH}_{\mathrm{ref}}(t) = 8$. A block diagram of the entire control system is shown in Fig. 5.

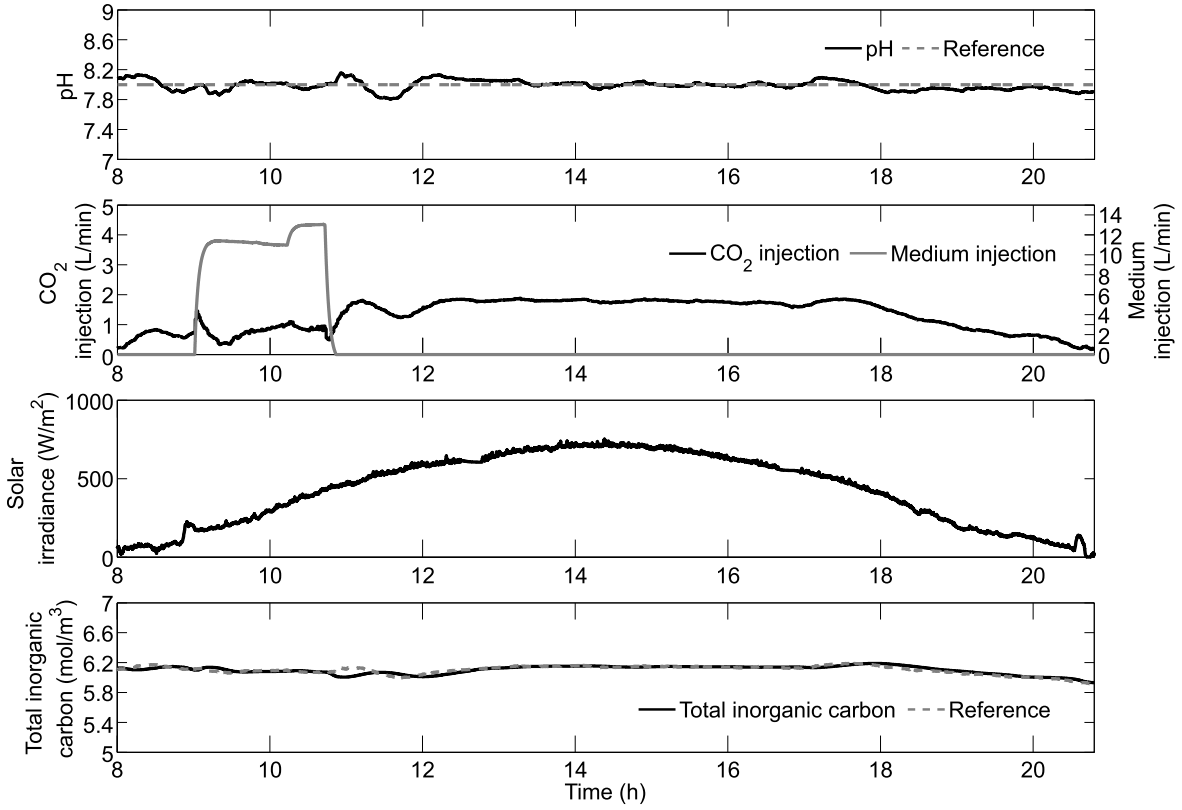

Fig. 7. Experimental results July 1, 2014.

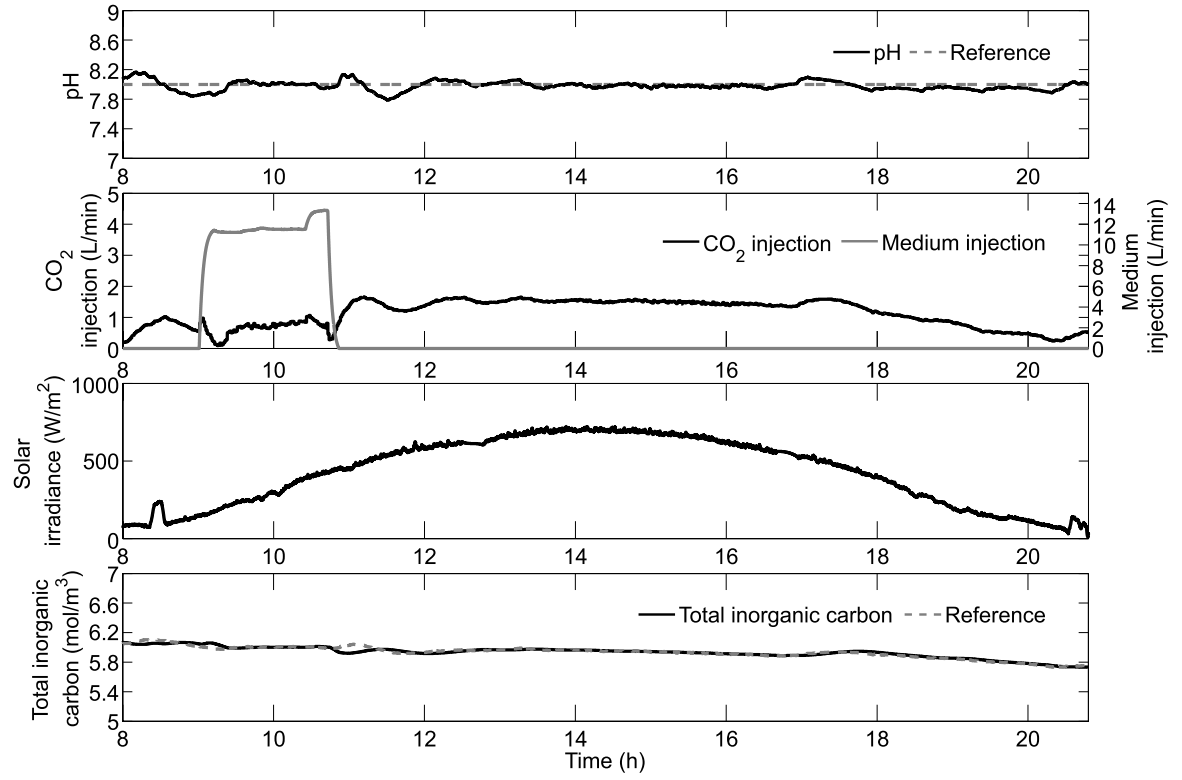

Fig. 8. Experimental results July 3, 2014.

For a constant set-point $[C_T]_{\text{ref}}(L,t)$ (calculated by the PI controller), the set-point profile $[C_T]_{\text{ref}}(x,t)$ is obtained from (40), which is a steady-state solution of the total inorganic carbon. This set-point profile is modified to obtain a perfect match between the desired pH_{ref} and the pH of the plant.

The design of the PI controller of the outer feedback loop was based on the Approximate M-constrained Integral Gain Optimisation (AMIGO) tuning rule [35]. This tuning rule methodology is based on a first-order transfer function plus dead time of the system. Thus, the reaction curve method based on an open-loop test [35] was used to calculate such model. In this way, during the night period of the day, where the solar irradiance does not affect the system, a step change at the total inorganic carbon reference was applied to capture the dynamics between the total inorganic carbon and the pH, as shown in Fig. 6. For this experiment, the inner DSMC-photobioreactor closed-loop system was considered.

As can be observed in Fig. 6, the increase in the total inorganic carbon produces a decrease in the pH, observing a time delay of 390 s. The evolution of the pH response is governed by two main dynamics [8], one second-order oscillatory term (natural frequency $\omega_n = 0.0140$ rad/s and relative damping factor $\xi = 0.0420$) and the other overdamped dynamic (with time constant 450 s). The fraction of the remaining injected CO_2 is recirculated producing the oscillatory behavior in the measured pH. However, to design the PI controller only the overdamped dynamic is considered. Then, the following first-order model with dead time, relating the pH output to the total inorganic carbon input, is obtained:

$$G(s) = \frac{-1.59}{450s + 1} e^{-390s} \tag{38}$$

where s is the Laplace operator. The resulting PI parameters, using the AMIGO tuning rule, are $k_p = -0.1778$ (m^3 L)/(mol min) and $T_i = 547.9434$ s.

In Fig. 7, the response of the sliding mode controller on July 1, 2014 is shown. The experiment lasted around 12:30 h. Between 09:00 and 11:00 h, the harvesting of the culture was performed, where fresh medium is injected in the photobioreactor. The controller responds by decreasing the carbon dioxide injection. It can be observed in the bottom graph of Fig. 7 that the total inorganic carbon remains constant along the day in such a way that the pH of the photobioreactor tracks the reference. Smooth changes in irradiance are about 100 W/m^2 and the controller compensates it in such a way that no tracking errors (more than ± 0.1) were found.

Another experiment performed on July 3, 2014 is shown in Fig. 8. The harvesting operation was performed between 09:00 and 11:00 h. The controller was regulating the dioxide carbon correctly flow during the whole test. In spite of the disturbances, the system response is smooth and the tracking error was less than ± 0.1 for the pH. This is a promising result, taking into account the disturbances affecting the plant and the uncertainties present in the system model.

V. Conclusion

This paper describes the development of a DSMC controller to regulate the pH of a tubular photobioreactor using the total inorganic carbon as the output of the process. The central idea of the control approach is the combination of the method of characteristics and SMC. The method of characteristics is employed for a general first-order PDE system to derive a nonlinear ODE system, which exactly describes the original PDE system. Then, the control design is performed in the ODE system instead of the original PDEs, which means that all known results for the description of sliding regimes in the control theory of lumped parameter systems become available for the PDE control problem. This approach was first proposed in [19].

Since the photobioreactor system has a relative degree 2, a second-order sliding manifold was developed, based on [18]–[20], to create a local sliding regime in the sliding surface.

The automatic control system developed was tested by simulations and implemented in an experimental plant, showing that the results satisfy the pH control objective better than a PI controller with feedforward scheme. Moreover, the use of the total inorganic carbon as output to control the pH of the system facilitates the derivation of the control law, under the hypothesis that carbon consumed by microalgae is compensated by supplying CO_2 to maintain pH, and as a consequence, a desired level of inorganic carbon is achieved.

Appendix
Derivation of the Control Law

In this appendix, the design of the continuous control law, based on the SMC methodology of Section III, to control the photobioreactor system is presented.

The sliding surface is chosen to be

$$h = ([C_T](x,t) - [C_T]_{\text{ref}}(x,t)) + \frac{1}{T_i}\int_0^t \langle [C_T] - [C_T]_{\text{ref}} \rangle d\sigma \tag{39}$$

where T_i is the time constant of the integral term, $[C_T]_{\text{ref}}(x,t)$ is the total inorganic carbon reference profile, and $\langle \cdot \rangle$ is the mean value of its arguments. The reference profile $[C_T]_{\text{ref}}(x,t)$ for this control strategy is calculated as

$$[C_T]_{\text{ref}}(x,t) = [C_T](0,t) + \delta(x)([C_T]_{\text{ref}}(L,t) - [C_T](0,t)) \tag{40}$$

where $\delta(x) = a\exp(bx)$ is a spatial-dependent function valid for $x \in [0, L]$, where $a = 0.039$ and $b = -0.014$. The $[C_T](0,t)$ value is directly obtained from the state observer. Equation (40) is used to compute the set-point profile in the DSMC control law. This expression was obtained by fitting the steady-state numerical solution of (3) over the photobioreactor operating point.

The control law is based on (36), which must be solved for $u \triangleq V_g$. It uses the two sets of characteristic vector fields to define the equivalent sliding dynamics. Evaluating such equation, it is obtained

$$\begin{aligned}(L_{\kappa_{2,u}}(L_{\kappa_1}h + \lambda_1 h)) + \lambda_2(L_{\kappa_1}h + \lambda_1 h) \\ = \frac{\partial^2 h}{\partial t^2} + V_l u\frac{\partial^2 h}{\partial x^2} + (V_l + u)\frac{\partial^2 h}{\partial t \partial x} + \tilde{\lambda}_1\left(\frac{\partial h}{\partial t} + u\frac{\partial h}{\partial x}\right) \\ + \tilde{\lambda}_2\left(\frac{\partial h}{\partial t} + V_l\frac{\partial h}{\partial x}\right) + \tilde{\lambda}_1\tilde{\lambda}_2 h = 0\end{aligned} \tag{41}$$

where $\tilde{\lambda}_1 = (1/4)\lambda_1$ and $\tilde{\lambda}_2 = (1/3)\lambda_2$. Substituting h into (41) yields

$$\begin{aligned}
&\frac{\partial^2[C_T]}{\partial t^2} + (u+V_l)\frac{\partial^2[C_T]}{\partial t\partial x} + uV_l\frac{\partial^2[C_T]}{\partial x^2} \\
&\quad - uV_l\frac{\partial^2[C_T]_{\text{ref}}}{\partial x^2} + \frac{1}{T_i}\frac{\partial[C_T]}{\partial t} + u\left(\frac{\partial[C_T]}{\partial x} - \frac{\partial[C_T]_{\text{ref}}}{\partial x}\right) \\
&\quad + \tilde{\lambda}_1\left[\frac{\partial[C_T]}{\partial t} + \frac{1}{T_i}([C_T]-[C_T]_{\text{ref}})\right. \\
&\qquad \left. + u\left(\frac{\partial[C_T]}{\partial x} - \frac{\partial[C_T]_{\text{ref}}}{\partial x}\right)\right] \\
&\quad + \tilde{\lambda}_2\left[\frac{\partial[C_T]}{\partial t} + \frac{1}{T_i}([C_T]-[C_T]_{\text{ref}})\right. \\
&\qquad \left. + V_l\left(\frac{\partial[C_T]}{\partial x} - \frac{\partial[C_T]_{\text{ref}}}{\partial x}\right)\right] + \tilde{\lambda}_1\tilde{\lambda}_2 \\
&\quad \times\left[[C_T]-[C_T]_{\text{ref}} + \frac{1}{T_i}\int_0^t\langle[C_T]-[C_T]_{\text{ref}}\rangle dt\right] = 0. \quad (42)
\end{aligned}$$

Note that the first three terms in (42) can be expressed by the Lie derivative of $[C_T]$ with respect to the two characteristic fields

$$\begin{aligned}
&L_{\kappa_2}(L_{\kappa_1}[C_T]) \\
&\quad = \frac{\partial^2[C_T]}{\partial t^2} + uV_l\frac{\partial^2[C_T]}{\partial x^2} + (u+V_l)\frac{\partial^2[C_T]}{\partial t\partial x} \\
&\quad = K_{la_l,\text{CO}_2}\left[\frac{\partial[\text{CO}_2]}{\partial t} + u\frac{\partial[\text{CO}_2]}{\partial x} + \frac{V_{\text{mol}}}{\varepsilon}(1-\varepsilon)\right. \\
&\qquad \left. \times K_{la_l,\text{CO}_2}\text{H}_{\text{CO}_2}P_T\left(\left[\text{CO}_2^*\right]-[\text{CO}_2]\right)\right] \\
&\qquad - \frac{P_{\text{CO}_2}}{M_{\text{CO}_2}}\left(u\frac{\partial C_b}{\partial x} + \frac{\partial C_b}{\partial t}\right). \quad (43)
\end{aligned}$$

Substituting (43) in (42), the following control law is obtained:

$$\begin{aligned}
u = &\left\{K_{la_l,\text{CO}_2}\right. \\
&\times\left[\text{H}_{\text{CO}_2}P_T\frac{V_{\text{mol}}}{\varepsilon}(1-\varepsilon)K_{la_l,\text{CO}_2}\left(\left[\text{CO}_2^*\right]-[\text{CO}_2]\right)+\beta_2\right] \\
&+\tilde{\lambda}_2\left[\frac{P_{\text{CO}_2}C_b}{M_{\text{CO}_2}}+K_{la_l,\text{CO}_2}\left(\left[\text{CO}_2^*\right]-[\text{CO}_2]\right)-V_l\frac{\partial[C_T]_{\text{ref}}}{\partial x}\right] \\
&+\left(\tilde{\lambda}_1\tilde{\lambda}_2+\frac{\tilde{\lambda}_1+\tilde{\lambda}_2}{T_i}\right)([C_T]-[C_T]_{\text{ref}})+\tilde{\lambda}_1\beta_1+\frac{\tilde{\lambda}_1\tilde{\lambda}_2}{T_i} \\
&\times\left.\int_0^t\langle[C_T]-[C_T]_{\text{ref}}\rangle dt - \frac{P_{\text{CO}_2}}{M_{\text{CO}_2}}\beta_3 + \frac{1}{T_i}\frac{\partial[C_T]}{\partial x}\right\}\Bigg/ \\
&\times\left\{\frac{P_{\text{CO}_2}}{M_{\text{CO}_2}}\frac{\partial C_b}{\partial x} + V_l\frac{\partial^2[C_T]_{\text{ref}}}{\partial x^2} - K_{a,\text{CO}_2}\frac{\partial[\text{CO}_2]}{\partial x}\right. \\
&\left.-\tilde{\lambda}_1\left[\frac{\partial[C_T]}{\partial x} - \frac{\partial[C_T]_{\text{ref}}}{\partial x}\right]\right\} \quad (44)
\end{aligned}$$

where

$$\begin{aligned}
\beta_1 &= -V_l\frac{\partial[C_T]}{\partial x} + \frac{P_{\text{CO}_2}C_b}{M_{\text{CO}_2}} + K_{la_l,\text{CO}_2}\left(\left[\text{CO}_2^*\right]-[\text{CO}_2]\right) \\
\beta_2 &= \frac{\beta_1}{P_2 - [\text{CO}_2]P_1P_3} \\
\beta_3 &= -V_l\frac{\partial C_b}{\partial x} + P_{\text{O}_2}C_bY_{p/x}.
\end{aligned}$$

To avoid the requirement of setting the slope of the total inorganic carbon profile set-point along the photobioreactor tube, (44) is integrated with respect to space. This results in the following final control law:

$$\begin{aligned}
u = &\left\{K_{la_l,\text{CO}_2}\right. \\
&\times\left[\text{H}_{\text{CO}_2}P_T\frac{V_{\text{mol}}}{\varepsilon}(1-\varepsilon)K_{la_l,\text{CO}_2}\left\langle\left[\text{CO}_2^*\right]-[\text{CO}_2]\right\rangle+\langle\beta_2\rangle\right] \\
&+\tilde{\lambda}_2\left[\frac{P_{\text{CO}_2}\langle C_b\rangle}{M_{\text{CO}_2}}+K_{la_l,\text{CO}_2}\left\langle\left[\text{CO}_2^*\right]-[\text{CO}_2]\right\rangle\right. \\
&\qquad \left.-V_l[C_T]_{\text{ref}}|_0^L\right]+\left(\tilde{\lambda}_1\tilde{\lambda}_2+\frac{\tilde{\lambda}_1+\tilde{\lambda}_2}{T_i}\right) \\
&\times\langle[C_T]-[C_T]_{\text{ref}}\rangle+\tilde{\lambda}_1\langle\beta_1\rangle+\frac{\tilde{\lambda}_1\tilde{\lambda}_2}{T_i} \\
&\times\left.\int_0^t\langle[C_T]-[C_T]_{\text{ref}}\rangle dt - \frac{P_{\text{CO}_2}}{M_{\text{CO}_2}}\langle\beta_3\rangle + \frac{1}{T_i}[C_T]|_0^L\right\}\Bigg/ \\
&\times\left\{\frac{P_{\text{CO}_2}}{M_{\text{CO}_2}}C_b|_0^L + V_l\left.\frac{\partial[C_T]_{\text{ref}}}{\partial x}\right|_0^L - K_{a,\text{CO}_2}\,[\text{CO}_2]|_0^L\right. \\
&\left.-\tilde{\lambda}_1([C_T]-[C_T]_{\text{ref}})|_0^L\right\}. \quad (45)
\end{aligned}$$

It is noteworthy that despite the fact that the control design is based on the theory of sliding modes, the implemented control law is continuous, hence avoiding the undesirable chattering effect of the SMC. Moreover, for implementation purposes, the derivative terms of the control law (45) were discretized by a backward finite difference scheme.

ACKNOWLEDGMENT

The authors would like to thank R. Cristiano for comments to improve the quality of this paper.

REFERENCES

[1] D. Chiaramonti *et al.*, "Review of energy balance in raceway ponds for microalgae cultivation: Re-thinking a traditional system is possible," *Appl. Energy*, vol. 102, pp. 101–111, Feb. 2013.

[2] O. Bernard, "Hurdles and challenges for modelling and control of microalgae for CO_2 mitigation and biofuel production," *J. Process Control*, vol. 21, no. 10, pp. 1378–1389, 2011.

[3] Y. Chisti, "Biodiesel from microalgae," *Biotechnol. Adv.*, vol. 25, no. 3, pp. 294–306, 2007.

[4] R. H. Wijffels and M. J. Barbosa, "An outlook on microalgal biofuels," *Science*, vol. 329, no. 5993, pp. 796–799, 2010.

[5] L. Brennan and P. Owende, "Biofuels from microalgae—A review of technologies for production, processing, and extractions of biofuels and co-products," *Renew. Sustain. Energy Rev.*, no. 14, no. 2, pp. 557–577, 2010.

[6] F. G. Acién Fernández, C. V. González-López, J. M. Fernández Sevilla, and E. Molina Grima, "Conversion of CO_2 into biomass by microalgae: How realistic a contribution may it be to significant CO_2 removal?" *Appl. Microbiol. Biotechnol.*, vol. 96, no. 3, pp. 577–586, 2012.

[7] F. G. Acién Fernández, F. García Camacho, J. A. Sánchez Pérez, J. M. Fernández Sevilla, and E. Molina Grima, "Modeling of biomass productivity in tubular photobioreactors for microalgal cultures: Effects of dilution rate, tube diameter, and solar irradiance," *Biotechnol. Bioeng.*, vol. 58, no. 6, pp. 605–616, 1998.

[8] M. Berenguel, F. Rodríguez, F. G. Acién, and J. L. García, "Model predictive control of pH in tubular photobioreactors," *J. Process Control*, vol. 14, no. 4, pp. 377–387, 2004.

[9] I. Fernández Sedano, J. Peña Martín, J. L. Guzman, M. Berenguel, and F. G. Acién Fernández, "Modelling and control issues of pH in tubular photobioreactors," in *Proc. 11th IFAC Symp. Comput. Appl. Biotechnol.*, Leuven, Belgium, 2010, pp. 186–191.

[10] M. R. Buehner *et al.*, "Microalgae growth modeling and control for a vertical flat panel photobioreactor," in *Proc. Amer. Control Conf.*, St. Louis, MO, USA, Jun. 2009, pp. 2301–2306.
[11] J. M. Romero-García, J. L. Guzmán, J. C. Moreno, F. G. Acién, and J. M. Fernández-Sevilla, "Filtered Smith predictor to control pH during enzymatic hydrolysis of microalgae to produce L-aminoacids concentrates," *Chem. Eng. Sci.*, vol. 82, pp. 121–131, Sep. 2012.
[12] A. Pawlowski, I. Fernández, J. L. Guzmán, M. Berenguel, F. G. Acién, and J. E. Normey-Rico, "Event-based predictive control of pH in tubular photobioreactors," *Comput. Chem. Eng.*, vol. 65, pp. 28–39, Jun. 2014.
[13] P. D. Christofides and P. Daoutidis, "Robust control of hyperbolic PDE systems," *Chem. Eng. Sci.*, vol. 53, no. 1, pp. 85–105, 1998.
[14] J.-J. Liu and J.-M. Wang, "Active disturbance rejection control and sliding mode control of one-dimensional unstable heat equation with boundary uncertainties," *IMA J. Math. Control Inf.*, vol. 32, no. 1, pp. 97–117, 2015.
[15] J.-M. Wang, J.-J. Liu, B. Ren, and J. Chen, "Sliding mode control to stabilization of cascaded heat PDE–ODE systems subject to boundary control matched disturbance," *Automatica*, vol. 52, no. 1, pp. 23–34, 2015.
[16] P. D. Christofides and P. Daoutidis, "Distributed output feedback control of two-time-scale hyperbolic PDE systems," *Appl. Math. Comput. Sci.*, vol. 8, no. 4, pp. 713–732, 1998.
[17] I. Fernández, F. G. Acién, M. Berenguel, and J. L. Guzmán, "First principles model of a tubular photobioreactor for microalgal production," *Ind. Eng. Chem. Res.*, vol. 53, no. 27, pp. 11121–11136, 2014.
[18] E. M. Hanczyc and A. Palazoglu, "Nonlinear control of a distributed parameter process: The case of multiple characteristics," *Ind. Eng. Chem. Res.*, vol. 34, no. 12, pp. 4406–4412, 1995.
[19] H. Sira-Ramirez, "Distributed sliding mode control in systems described by quasilinear partial differential equations," *Syst. Control Lett.*, vol. 13, pp. 177–181, Jul. 1989.
[20] E. M. Hanczyc and A. Palazoglu, "Sliding mode control of nonlinear distributed parameter chemical processes," *Ind. Eng. Chem. Res.*, vol. 34, no. 2, pp. 557–566, 1994.
[21] G. Andrade, D. J. Pagano, I. Fernández Sedano, J. L. Guzman, and M. Berenguel, "Boundary control of an industrial tubular photobioreactor using sliding mode control," in *Proc. 19th World Congr. Int. Fed. Automat. Control*, Cape Town, South Africa, 2014, pp. 4903–4908.
[22] H. Sira-Ramirez, "Nonlinear variable structure systems in sliding mode: The general case," *IEEE Trans. Autom. Control*, vol. 34, no. 11, pp. 1186–1188, Nov. 1989.
[23] J.-J. E. Slotine and W. Li, *Applied Nonlinear Control*. Englewood Cliffs, NJ, USA: Prentice-Hall, 1991.
[24] H. Shang, J. F. Forbes, and M. Guay, "Feedback control of hyperbolic distributed parameter systems," *Chem. Eng. Sci.*, vol. 60, no. 4, pp. 969–980, 2005.
[25] J. Y. Hung, W. Gao, and J. C. Hung, "Variable structure control: A survey," *IEEE Trans. Ind. Electron.*, vol. 40, no. 1, pp. 2–22, Feb. 1993.
[26] J. F. Sánchez, J. M. Fernández, F. G. Acién, A. Rueda, J. Pérez-Parra, and E. Molina, "Influence of culture conditions on the productivity and lutein content of the new strain *Scenedesmus almeriensis*," *Process Biochem.*, vol. 43, no. 4, pp. 398–405, 2008.
[27] I. Fernández, F. G. Acién, J. M. Fernández, J. L. Guzmán, J. J. Magán, and M. Berenguel, "Dynamic model of microalgal production in tubular photobioreactors," *Bioresour. Technol.*, vol. 126, pp. 172–181, Dec. 2012.
[28] F. Camacho Rubio, F. G. Acién Fernández, J. A. Sánchez Pérez, F. García Camacho, and E. Molina Grima, "Prediction of dissolved oxygen and carbon dioxide concentration profiles in tubular photobioreactors for microalgal culture," *Biotechnol. Bioeng.*, vol. 62, pp. 71–86, Jan. 1999.
[29] F. John, *Partial Differential Equations*. New York, NY, USA: Springer-Verlag, 1981.
[30] V. I. Arnold, *Geometrical Methods in the Theory of Ordinary Differential Equations*. London, U.K.: Springer-Verlag, 1983.
[31] V. I. Utkin, *Sliding Modes and Their Application in Variable Structure Systems*. Moscow, Russia: MIR Publishers, 1978.
[32] K. D. Young, V. I. Utkin, and U. Ozguner, "A control engineer's guide to sliding mode control," *IEEE Trans. Control Syst. Technol.*, vol. 7, no. 3, pp. 328–342, May 1999.
[33] G. A. Andrade, D. J. Pagano, J. D. Álvarez, and M. Berenguel, "Sliding mode control of distributed parameter processes: Application to a solar power plant," *J. Control, Autom., Elect. Syst.*, vol. 25, no. 3, pp. 291–302, 2014.
[34] A. F. Filippov, *Differential Equations With Discontinuous Righthand Sides*. Dordrecht, The Netherlands: Kluwer, 1988.
[35] K. J. Åström and T. Hägglund, *Advanced PID Control*. Research Triangle Park, NC, USA: ISA, 2005.

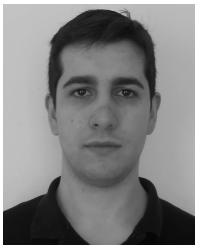

Gustavo A. de Andrade is currently pursuing the Ph.D. degree with the Department of Automation and Systems, Federal University of Santa Catarina, Florianópolis, Brazil.

His current research interests include control theory, distributed parameter systems, and optimization.

Daniel J. Pagano was born in La Plata, Argentine, in 1961. He received the B.Sc. degree in telecommunications engineering from the National University of La Plata, La Plata, in 1985, the M.Sc. degree in electrical engineering from the Federal University of Santa Catarina, Florianópolis, Brazil, in 1989, and the Ph.D. degree in robotics, automation and electronics from the University of Seville, Sevilla, Spain, in 1999.

He is currently a Professor with the Department of Automation and Systems, Federal University of Santa Catarina. His current research interests include nonlinear dynamical systems, bifurcation analysis, nonlinear control, power electronics, microgrids, and their applications.

José Luis Guzmán received the Computer Science Engineering and European Ph.D. degrees from the University of Almería, Almería, Spain, in 2002 and 2006, respectively.

He is currently an Associate Professor of Automatic Control and Systems Engineering with the University of Almería. His current research interests include the fields of control education, MPC techniques, PID control, and robust control with applications to agricultural processes, solar plants, and biotechnology.

Prof. Guzmán has been a member of the Spanish Association in Automatic Control CEA-IFAC since 2003, the IEEE Control System Society since 2006, and the IFAC Technical Committee on Control Education and the IEEE Technical Committee on System Identification and Adaptive Control since 2008. He received the Extraordinary Doctorate Award from the University of Almería.

Manuel Berenguel (A'01–M'04–SM'12) received the Industrial Engineering and Ph.D. degrees from the University of Seville, Seville, Spain, in 1992 and 1996, respectively.

He is currently a Full Professor of Automatic Control and Systems Engineering with the University of Almería, Almería, Spain. His current research interests include predictive, hierarchical, and robust control, with applications to solar energy systems, agriculture, and biotechnology, and control education through interactive tools and virtual/remote labs.

Prof. Berenguel has been a member of the Board of Governors of the Spanish Association of Automatic Control CEA-IFAC from 2003 to 2008 and since 2012. He has been a member of the IEEE Control System Society since 2000. He is a member of the IFAC Technical Committees TC 8.01 Control in Agriculture, TC 6.3. Power and Energy Systems, and TC 8.4 Biosystems and Bioprocesses. He received the Extraordinary Doctorate Award from the University of Seville.

Ignacio Fernández received the Computer Science Engineering and International Ph.D. degrees from the University of Almería, Almería, Spain, in 2009 and 2014, respectively.

He is currently a Research Member with the Automatic, Robotic and Mechatronic Research Group, University of Almería. His current research interests include system modeling and identification, MPC techniques, PID control, and control education with applications to agricultural processes, solar plants, and biotechnology.

Francisco Gabriel Acién received the Chemical Engineering degree from the University of Granada, Granada, Spain, in 1992, and the Ph.D. degree from the University of Almería, Almería, Spain, in 1996.

He has been a Professor with the Department of Chemical Engineering, University of Almería, since 2012. His major contributions on biotechnology of microalgae field are related to the improvement of photobioreactors design, scale-up of production systems, and economic analysis of production processes. He has participated in ten European projects, in addition to 30 national projects and contracts with companies. He has authored over 90 papers in international journals and 12 book chapters, in addition to eight patents extended at international level.

Prof. Acién is a member of the International Society for Applied Phycology and the Latino American Society for Algal and Environmental Biotechnology, and an Editor of *Algal Research* and *RELABIAA* journals, in addition to reviewer of international journals.